FINAL REPORT

Anticorrosion Coatings Based on Assemblies of Superhydrophobic Particles Impregnated with Conductive Oil

SERDP Project WP-2524

MAY 2016

Polyzos Georgios
Vlassiouk Ivan
Sharma Jaswinder
Oak Ridge National Laboratory

SERDP
DOD ▪ EPA ▪ DOE

Page Intentionally Left Blank

Page Intentionally Left Blank

REPORT DOCUMENTATION PAGE

Form Approved
OMB No. 0704-0188

1. REPORT DATE *(DD-MM-YYYY)*	**2. REPORT TYPE**	**3. DATES COVERED** *(From - To)*
13/5/2016	Final Report	April 2015 – April 2016

4. TITLE AND SUBTITLE

Anticorrosion coatings based on assemblies of superhydrophobic particles impregnated with conductive oil

5a. CONTRACT NUMBER
WP-2524

5b. GRANT NUMBER

5c. PROGRAM ELEMENT NUMBER

6. AUTHOR(S)

Polyzos Georgios, Sharma Jaswinder, Vlassiouk Ivan

5d. PROJECT NUMBER

5e. TASK NUMBER

5f. WORK UNIT NUMBER

7. PERFORMING ORGANIZATION NAME(S) AND ADDRESS(ES)

Oak Ridge National Laboratory
One Bethel Valley Road
Oak Ridge, TN 37831-6054

8. PERFORMING ORGANIZATION REPORT NUMBER

9. SPONSORING / MONITORING AGENCY NAME(S) AND ADDRESS(ES)

Strategic Environmental
Development Program (SERDP)
4800 Mark Center Drive
Alexandria, VA 22350-3605

10. SPONSOR/MONITOR'S ACRONYM(S)
SERDP

11. SPONSOR/MONITOR'S REPORT NUMBER(S)

12. DISTRIBUTION / AVAILABILITY STATEMENT

Approved for public release; distribution is unlimited.

13. SUPPLEMENTARY NOTES

14. ABSTRACT

We developed low contact resistance passivate coatings for electrical system components. The coatings inhibited the build-up of resistive corrosion on electrical connector backshells as well as on steel components that are commonly used in electrical equipment. The developed coatings are based on assemblies of superhydrophobic diatomaceous earth and silica particles. To enhance the corrosion resistance and achieve low electrical resistance, exfoliated graphene sheets were dispersed in polydimethylsiloxane and the electrically conductive suspension was impregnated inside the porous patterns of the silica particles. The coatings can be applied to steel components, steel components coated with zinc-nickel and electrical connectors through an aerosol spray process. Corrosion in electronic components cannot be readily detected and is the predominant cause for electronic component failures when electrical equipment is exposed to environmental conditions. The developed coatings are inexpensive and scalable and can potentially be utilized to effectively protect critical infrastructure from corrosion. The developed coatings are compatible with coatings that are currently being used in electronic components (i.e. zinc-nickel).

15. SUBJECT TERMS
Anticorrosion, superhydrophobic, polydimethylsiloxane, graphene

16. SECURITY CLASSIFICATION OF:			**17. LIMITATION OF ABSTRACT**	**18. NUMBER OF PAGES**	**19a. NAME OF RESPONSIBLE PERSON**
a. REPORT	**b. ABSTRACT**	**c. THIS PAGE**			Polyzos Georgios
U	U	U	UU	23	**19b. TELEPHONE NUMBER** *(include area code)* 865-576-2348

Standard Form 298 (Rev. 8-98)
Prescribed by ANSI Std. Z39.18

Page Intentionally Left Blank

Table of Contents

List of Figures

List of Nomenclature and Acronyms

Symbol	Meaning
SH	Superhydrophobic
ZnNi	Zinc-Nickel
DE	Diatomaceous Earth
SEM	Scanning Electron Microscopy
TEOS	Tetraethyl Orthosilicate
ASTM	American Society for Testing and Materials
GnPs	Graphene NanoPlatelets
CVD	Chemical vapor deposition
CA	Contact Angle
CC	Clear Coat

Keywords: Anticorrosion, superhydrophobic, polydimethylsiloxane, graphene

Acknowledgements: We wish to thank Dr. Nathan Wood from Oak Ridge National Laboratory for his help with the salt fog experiments.

Anticorrosion coatings based on assemblies of superhydrophobic particles impregnated with conductive oil

Abstract

Objectives: We developed low contact resistance passivate coatings for electrical system components. The coatings inhibited the build-up of resistive corrosion on electrical connector backshells as well as on steel components that are commonly used in electrical equipment. The coated components demonstrated superior corrosion resistance compared to the respective steel and ZnNi components.

Technical Approach: The developed coatings are based on assemblies of superhydrophobic diatomaceous earth and silica particles. To enhance the corrosion resistance and achieve low electrical resistance, exfoliated graphene sheets were dispersed in polydimethylsiloxane and the electrically conductive suspension was impregnated inside the porous patterns of the silica and diatomaceous earth particles. Amorphous silica nanoparticles were synthesized using sol-gel techniques. The particles were fluorinated to impart them with superhydrophobic properties. The graphene nanoplatelets were exfoliated using ultrasonic agitation and high-shear mixing techniques.

Results: The synergistic effects of the water repellency, and moisture and oxygen barrier resulted in an impermeable coating that protected metal components from corrosion (p*roof-of-concept*). The assemblies of graphene nanoplatelets, and superhydrophobic silica particles demonstrated excellent corrosion resistance. The samples retained their superhydrophobic properties and were corrosion free after 240 h of salt-fog testing.

Benefits: The coatings can be applied to steel components, steel components coated with zinc-nickel and electrical connectors through an aerosol spray process. Corrosion in electronic components cannot be readily detected and is the predominant cause for electronic component failures when electrical equipment is exposed to environmental conditions. The developed coatings are inexpensive and scalable and can potentially be utilized to effectively protect critical infrastructure from corrosion. The developed coatings are compatible with coatings that are currently being used in electronic components (i.e. zinc-nickel).

1. Objective

The objective of this SEED project was to develop low resistance coatings that can eliminate the use of hexavalent chromium and cadmium. Such coatings can reduce the overall hazardous waste and the worker exposure to toxic materials. We investigated the corrosion resistance mechanism of multifunctional coatings based on superhydrophobic (SH) silica and graphene particles. The outer surface of the coating was nanostructured with low surface energy materials in order to become SH and repel water. The SH layer is an effective barrier against bulk water. However, SH surfaces alone cannot prevent water vapor condensation on a surface. The condensed vapors

will ultimately penetrate through the coating layer and will initiate the build-up of corrosion. Moreover, SH coatings are porous and allow the oxygen permeation. In order to block the diffusion of water vapors and oxygen permeation, the bulk (volumetric) structure of the coating was filled with exfoliated graphene nanoplatelets (GnPs). The developed low-resistance coatings are compatible with zinc-nickel (ZnNi) and steel components. They can be applied on electrical connector backshells with ZnNi finish in order to impede the build-up of resistive corrosion and prolong the lifetime and performance of the connectors. The coatings can be applied using spray-coating techniques. The coated components were subjected to salt-fog testing according to ASTM B-117. In order to optimize the structure of the coatings particles with different sizes and geometries were utilized.

2. Background

Past research work in our group

Superhydrophobic (SH) surfaces have drawn significant scientific attention, as they can be a viable approach toward mitigating corrosion. Numerous methods have been proposed for fabricating SH surfaces [1-4]; however, large area SH surfaces are still underutilized due to their poor durability and inability to be scaled cost effectively. Our group has developed high-performance, environmentally friendly anticorrosion coatings based on diatomaceous earth (DE) particles. DE particles consist of intricately shaped silicified frustules with regular patterns of micro- and nano- pores. The fossilized frustules were nutrient sieves of living diatoms and their geometry and vesicle structure are species specific [5]. A common structure is shown in Figure 1. They are mainly formed by amorphous silicon dioxide (~95%) and trace elements such as magnesium and aluminum. The high porosity and large surface area of these fossilized skeletons provide a hydroxyl rich template on which low energy self-assembled monolayers of paraffinic- or fluoro-silanes (i.e. n-octadecyltrichlorosilane or tridecafluoro-1,1,2,2-tetrahydrooctyltrichlorosilane) can be covalently bonded. The resulting functionalized DE particles exhibit extreme water repellency properties with contact and rolling angles approximately 170^{o} and 3^{o}, respectively.

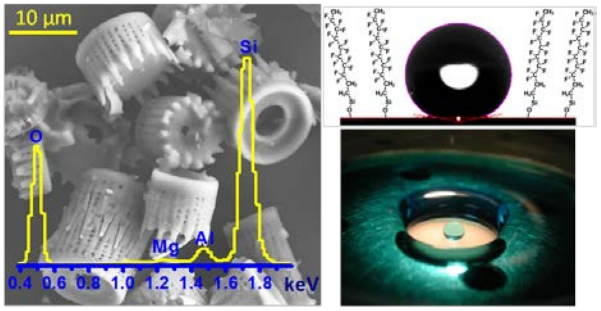

Figure 1. Scanning electron microscopy (SEM) image showing the structure of individual DE particles. Particles consist of 95wt% silicon dioxide and 5wt% aluminum and magnesium trace elements according to energy dispersive X-ray element analysis. Surfaces based on DE functionalized with low surface energy monolayers are extremely water repellent and exhibit water contact angle values of approximately 170^{o}.

Metallic test samples were coated with a colloidal suspension of superhydrophobic diatomaceous earth (SHDE) particles and organic binders using a spray deposition technique. Interparticle cohesive forces (mainly capillary forces caused by liquid bridges [6,7] during solvent evaporation) form particle assemblies on the surface of the plates. The structure of these SH assemblies depends on the colloidal particle size distribution. A typical particle distribution and the resulting SH surface are shown in Figure 2.

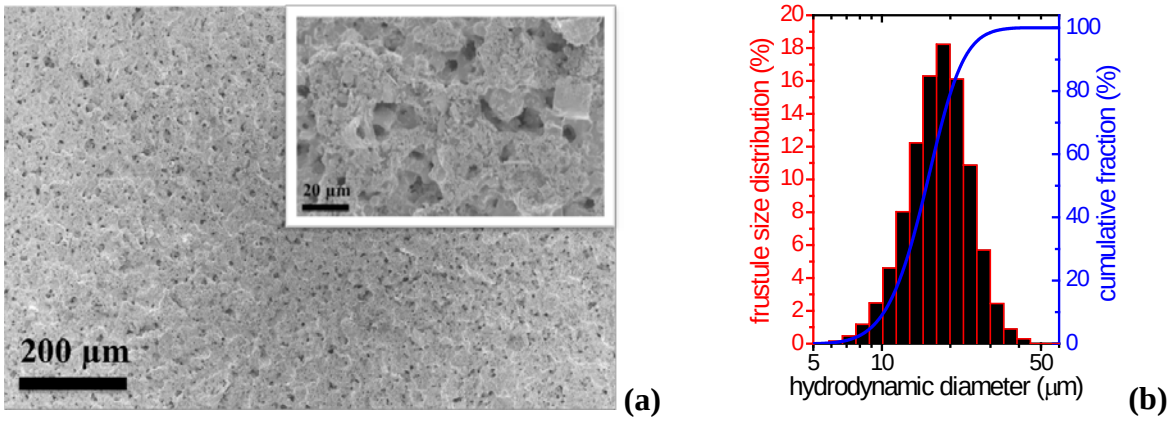

Figure 2. (a) SEM images of SHDE particle assemblies spray-deposited on a steel substrate. **(b)** The particle's median and mean values are 15.7 and 16.2µm, respectively.

Long-term environmental tests were conducted on coated carbon steel substrates. A suspension of SHDE particles and a polyurethane based binder (weight ratio 4:5) was spray-deposited on carbon steel plates that were previously coated with an organic primer. The studies were performed in an outdoor testing area for approximately 2 years, where the steel plates were directly exposed to East Tennessee, USA weathering conditions. The plates were lying in a nearly horizontal (2-5^{o}) elevation. Surface temperatures ranged from -10 ^{o}C to > 50 ^{o}C, with more than 125 cm of rain during this time. The plates were subjected to high relative humidity with early morning dew and condensation collecting on the plates almost daily. The corrosion formation was regularly monitored at various times after initial exposure and the condition of the plates is shown in Figure 3. After the first rainstorm, the uncoated plate that was used for control sample was entirely corroded in less than a month. The low surface energy of the DE coated sample resulted in considerable corrosion resistance. The first signs of corrosion became visible after 9 months and gradually progressed until the end of the experiments. This limited resistance is mainly associated with water condensation effects due to diffusion of water vapors through the micro and nano scale surface features. In order to enhance the corrosion resistance during high humidity environments, a dilute solution of high viscosity (100,000 cSt) polysiloxane oil was sprayed on the plates. The oil was impregnated inside the porous patterns of the diatomite surface leaving the outer surface of the coating oil-free. The cumulative contributions of the diatomite's low surface energy and of the polysiloxane barrier layer induced

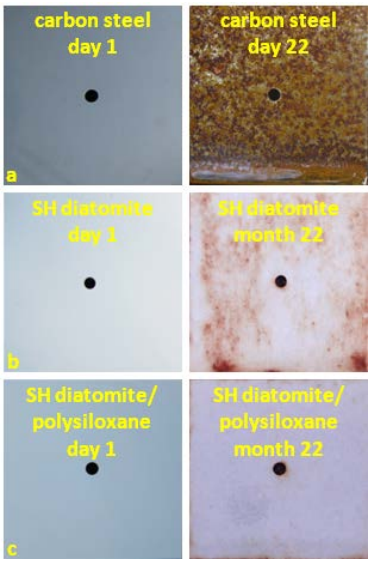

Figure 3. Corrosion resistance tests on carbon steel plates exposed to weathering conditions. **(a)** The uncoated plate was entirely corroded in the first 22 days. **(b)** The coating based on assembled SHDE particles, provided limited corrosion protection. **(c)** The synergistic effect between the nanostructured SH surface and the water vapor barrier layer due to the impregnated polysiloxane oil resulted in corrosion-free plates over the 22 months of outdoor exposure.

long-term anticorrosion resistance and plates were corrosion-free over the 22 months of weathering exposure.

The abrasion resistance of the coatings was tested using a Taber rotary platform. Rub-wear experiments were performed on samples turning against two abrading CS10 wheels with 75g load on each grinding wheel. The coatings retained their SH patterns with an average abrading rate of 18μm per 50 cycles. Further improvement in the abrading resistance can be achieved by grafting on the DE particle surface monolayers with coupling agents (binding sites, i.e. epoxide rings or amines) that can be covalently bonded to a polymeric binder. Depending on the chemical structure and the reaction kinetics of the assembled monolayers, the population and spatial distribution of the coupling agents can be controlled in order to provide binding sites on the surface of the diatomite frustules without sacrificing their SH properties.

3. Materials and Methods

Superhydrophobic particles

We synthesized and functionalized superhydrophobic silica particles with different sizes and geometries. The particles were functionalized in a solution of self-assembled monolayers of fluoro-silanes according to our previous studies [7]. Three types of particles were investigated:

i) Cylindrical DE particles (16 μm in size); *ii)* Spherical silica particles with diameter comparable to the size of DE particles; *iii)* Spherical silica particles with diameter smaller than 1 micron (approximately 300 nm). A representative energy dispersive X-Ray (EDX) spectrum and SEM images of the DE particles are shown in Figure 4. According to the element analysis the silica (SiO_2) content of the particles is approximately 85%. The particles were successfully functionalized with fluoro-silanes [7]. Moreover, spherical silica particle were synthesized in the lab using sol-gel techniques. The particles were synthesized in a solution of tetraethyl orthosilicate (TEOS) according to the following reaction:

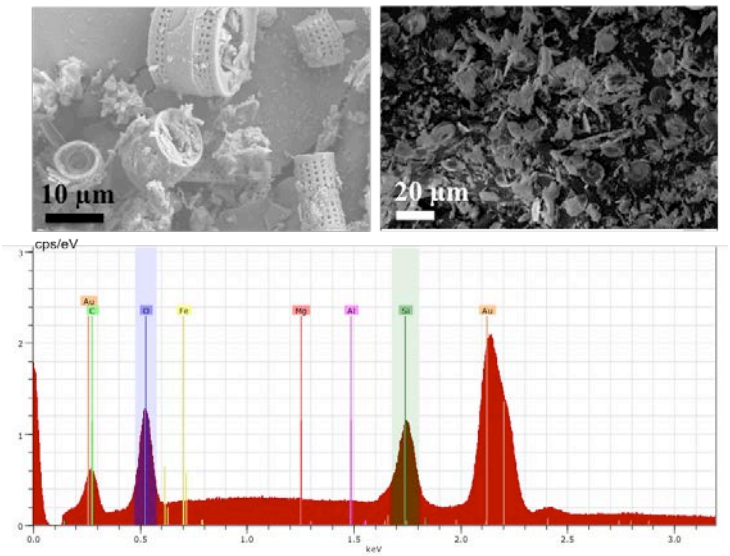

Figure 4. EDX spectrum and SEM images of the DE particles that were used in the fabrication of the coatings.

$$Si(OC_2H_5)_4 + 2\ H_2O \rightarrow SiO_2 + 4\ C_2H_5OH$$

SEM images of the synthesized particles are shown in Figure 5. In order to increase the surface area of the particles we introduced porous features on their surface. The size of the particles is uniform (monodispersed particles) and is approximately 300 nm. The silica particles were functionalized with fluoro-silanes. All functionalized particles (DE and sol-gel synthesized particles) demonstrated water repellent properties. The water contact angle (CA) values were higher than 160°.

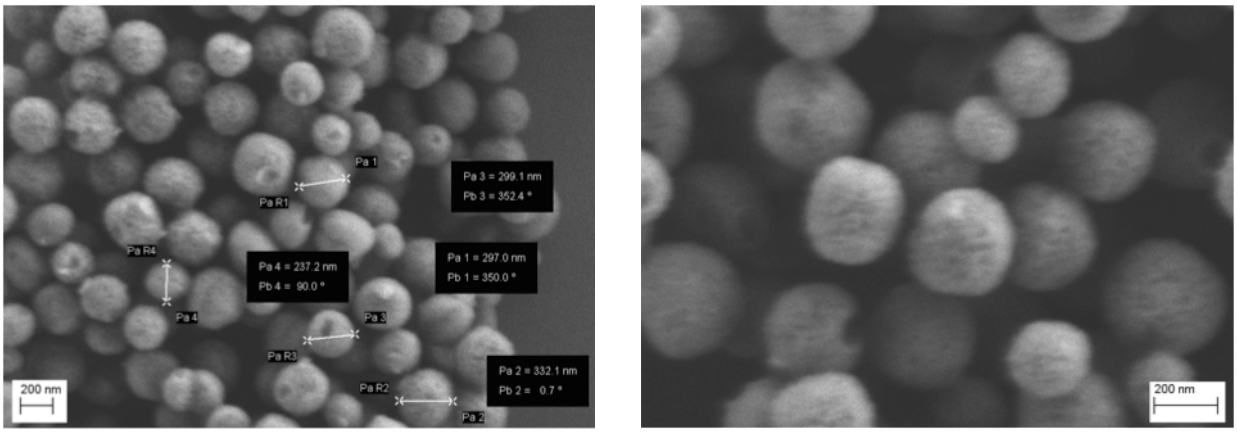

Figure 5. SEM images of porous silica particles of controlled size synthesized using sol-gel techniques.

Exfoliated graphene nanoplatelets

Exfoliated graphene nanoplatelets (GnPs) were obtained using ultrasonic agitation and high-shear mixing techniques [10]. Representative SEM images of the aggregated and exfoliated graphene platelets are shown in Figure 6. The GnPs were dispersed in polydimethylsiloxane oil and thereafter were impregnated into the superhydrophobic coatings through their porous features.

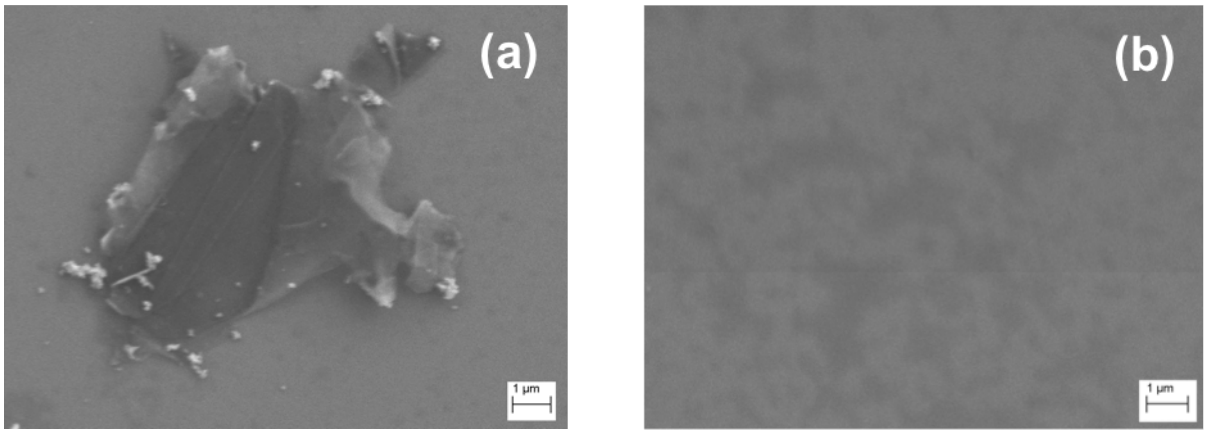

Figure 6. (a) Aggregated graphene platelet **(b)** exfoliated graphene nanoplatelets.

The developed coatings were applied onto electrical connectors and steel plates (1018) coated with 8 microns of ZnNi. The synthesized materials can be scaled to commercial quantities.

4. Results and Discussion

The developed coatings are multicomponent and consist of two different polymer binders, functionalized silica particles and exfoliated GnPs. In order to evaluate the corrosion resistance of the individual components, steel and aluminum plates were coated with the following combinations:

1) Uncoated steel plate; 2) steel plate coated with clear coat (CC) polymer binder; 3) steel plate coated with SHDE dispersed in CC; 4) steel plate coated with exfoliated GnPs dispersed in polydimethylsiloxane; 5) steel plate coated with SHDE dispersed in CC and exfoliated GnPs

dispersed in polydimethylsiloxane; 6) steel plate coated with polydimethylsiloxane; 7) aluminum plate coated with SHDE dispersed in CC and exfoliated GnPs dispersed in polydimethylsiloxane; 8) uncoated aluminum plate.

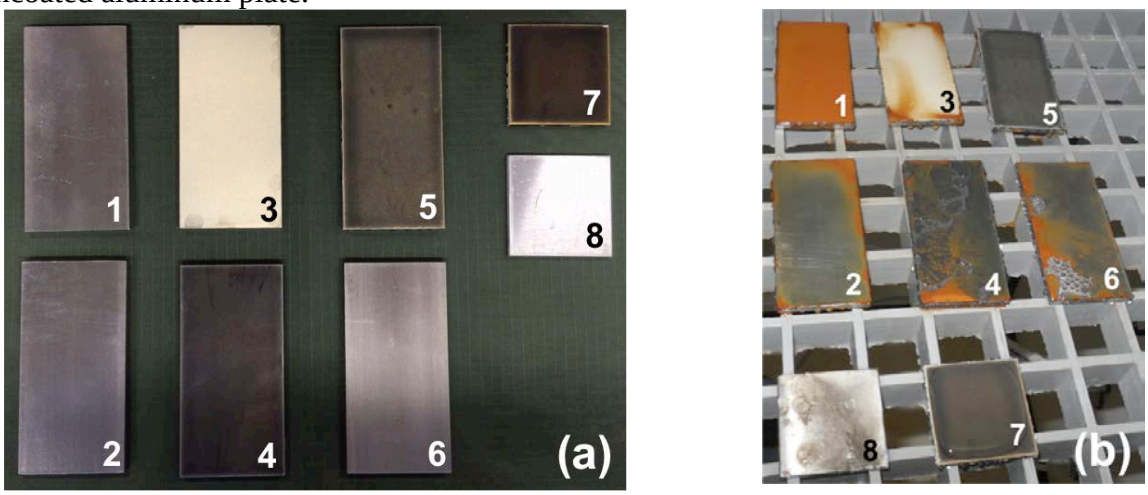

Figure 7. Steel (2x4 inch) and aluminum (1x1 inch) plates coated with polymer binders, SHDE and GnPs. **(a)** The plates before the salt-fog testing. **(b)** The plates after 72 h in the salt-fog chamber.

The plates were tested for 72 h in the salt-fog chamber (Figure 7). The uncoated steel (1) and aluminum (8) plates were entirely corroded. Plates 2, 3, 4, and 6 were partially corroded; whereas, plates 5 and 7 showed no sign of corrosion. Therefore, the combination of SH particles and GnPs resulted in coatings with enhanced corrosion resistance properties.

GnPs were dispersed into polydimethylsiloxane until the composite mixture became electrically conductive. Three series of coated samples were prepared based on conductive polydimethylsiloxane and i) cylindrical silica (16 µm), spherical silica (9 µm) and spherical silica (300 nm). The silica content varied in each series of samples. The coated plates and electrical connectors before the salt-fog testing are shown in Figure 8. The white color of the samples is due to the silica. The sample designation is as follows:

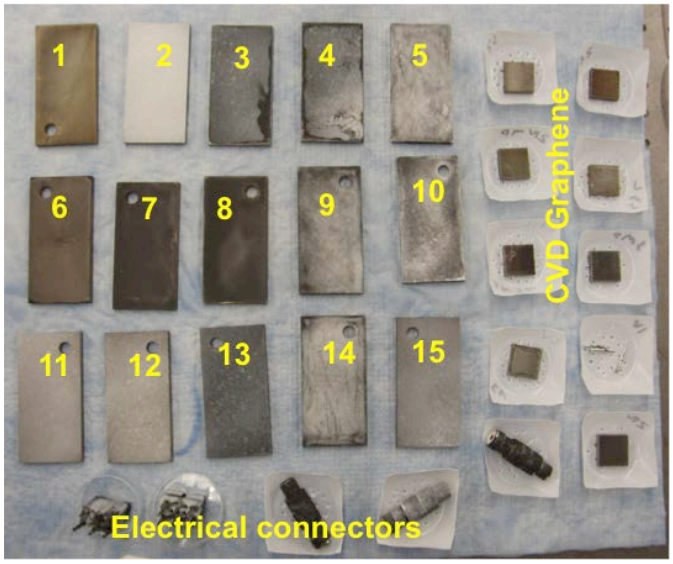

Figure 8. Coated samples before the salt-fog testing. ZnNi plates (2x4 inch) and electrical connectors coated with different formulations of polydimethylsiloxane , GnPs and SH silica particles. Single layers of graphene crystals were deposited on top of ZnNi plates (1x1 inch).

1: ZnNi; 2: 0.6g SHDE in 0.5g CC on steel; 3: 0.6g SH silica (9µm) in 0.5g CC and 1.2g polydimethylsiloxane with GnPs on steel; 4,5: 0.6g SH silica (9µm) in 0.5g CC and 1.2g polydimethylsiloxane with GnPs on steel; 6: 0.3g SH silica (300nm) in 0.2g CC and 0.6g polydimethylsiloxane with GnPs on ZnNi; 7,8: 0.6g SH silica (300nm) in 0.5g CC and 1.2g

polydimethylsiloxane with GnPs on ZnNi; 9,10: 0.6g SH silica (9μm) in 0.5g CC and 1.2g polydimethylsiloxane with GnPs on ZnNi; 11,12: 0.6g SH silica (9μm) in 0.5g CC and 1.2g polydimethylsiloxane with GnPs on ZnNi; 13: 0.8g SH silica (300nm) in 0.6g CC and 1.2g polydimethylsiloxane with GnPs on ZnNi; 14,15: 0.6g SH silica (9μm) in 0.5g CC and 1.2g polydimethylsiloxane with GnPs on ZnNi.

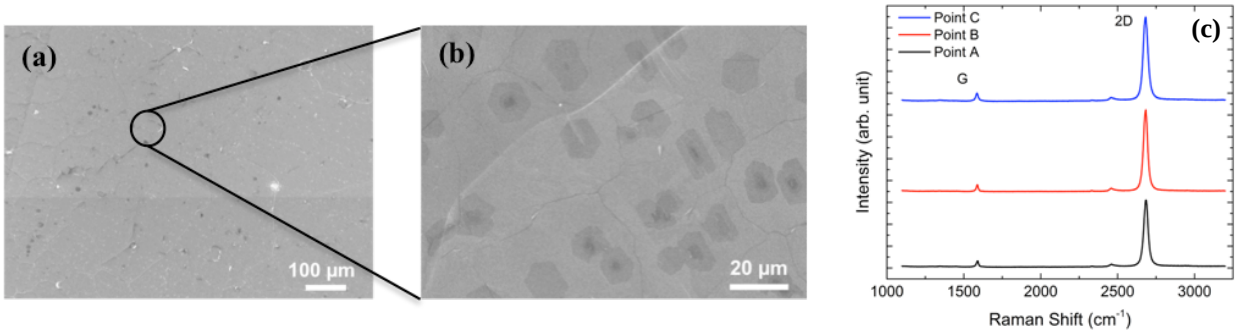

Figure 9. (a),(b) SEM images at low and high magnifications of graphene synthesized using chemical vapor deposition techniques. **(c)** Raman spectra at three different points of a graphene single layer.

We investigated the corrosion mechanism of the coating that was based on exfoliated GnPs with no SH silica (sample 4 in Figure 7). Graphene is an absolute barrier to oxygen and moisture and therefore a possible supposition for the corrosion mechanism is the finite size of the GnPs. Oxygen and moisture may diffuse through the tortuous paths that are formed around the exfoliated GnPs and corrode the metallic substrate. To investigate the factors that may be associated with the corrosion mechanism, a second series of samples was developed. These samples are shown in Figure 8 and are made of continuous layers of graphene. The geometrical configuration does not form tortuous paths. Chemical vapor deposition (CVD) techniques were utilized to grow continuous single layer graphene crystals (one atom thick). The experimental procedure is described in our previous studies [8,9]. Representative SEM images of a graphene layer that was synthesized using CVD techniques are shown in Figure 9. The graphene layer is continuous according to the low magnification image (Figure 9a). Higher magnification images were used to study the structure of the crystal's surface. In Figure 9b the hexagonal patterns are due to the bilayer crystals that reside on top of the single crystal. The estimation of the layer thickness can be performed using Raman spectroscopy. The Raman spectra at three different points on the crystal's surface are shown in Figure 9c. The shape and the intensity ratio of the 2D and G peaks indicate that the thickness of the measured points corresponds to a single atom. Details on the spectra analysis and thickness determination can be found in reference [11].

The single atom graphene layers were transferred onto 1x1 inch ZnNi plates (steel plates coated with 8μm ZnNi). On each plate three single layers were deposited. Seven plates were tested. The plates are shown in Figure 7 and

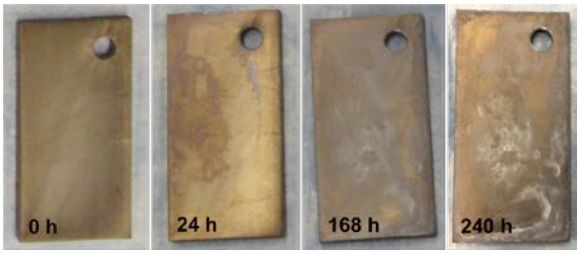

Figure 10. ZnNi plate before testing and after 24, 168, and 240 h in the salt-fog chamber.

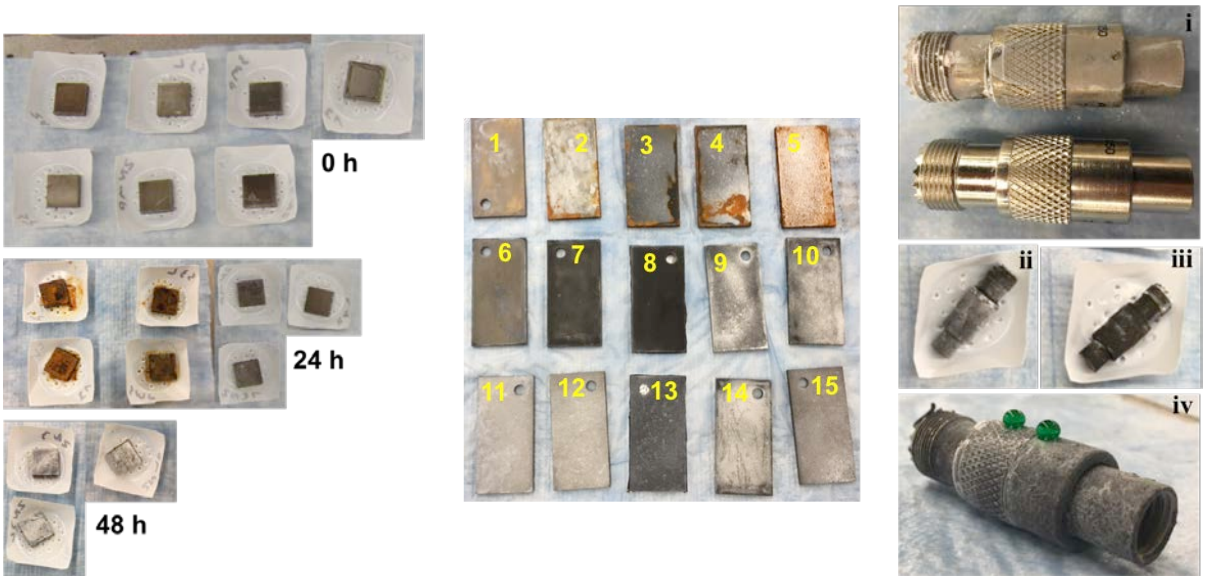

Figure 11. (a) The CVD graphene samples. After 48 h of testing all samples were corroded. The corrosion mechanism was accelerated compared to the pristine ZnNi sample in Figure 10. **(b)** Coated plates after 240 h of testing. Plates 6-15 have no sign of corrosion. Plates 6,7,8, and 13 are electrically conductive. Among all the developed formulations these are the best performing coatings. **(c) i)** Backshell electrical connectors before and after 240 h of testing. After 240 h of testing the uncoated connector is corroded and non-conductive. **ii, iii)** Coated backshell connectors after 240 h of testing. No sign of corrosion are observed. The coatings of the connectors shown in images ii and iii are the same with the coatings of the plates 7 and 13, respectively. **iv)** Water droplets on top of the connector shown in image ii after 240 h of testing. The connector retained its superhydrophobic properties. The white color is due to the silica component of the coating.

are designated as CVD graphene. The sides of all samples were coated in order to inhibit the corrosion formation through the side defects. The sides of the CVD graphene samples were coated with epoxy resin. After each test cycle and prior to the sample evaluation, the samples were removed from the salt-fog chamber, washed with copious amounts of water to remove the salt residuals on their surface and dried at 50 ^{o}C for 6 h. In Figure 10 are shown the uncoated ZnNi (baseline) sample (plate 1 in Figure 8). The thickness of the ZnNi layer is 8 μm. The sample started to discolor after 24 h salt-fog testing. After 240 h of testing the sample was significantly corroded and non-conductive. In the remainder of the report, the corrosion resistance of the developed coatings is compared against the corrosion resistance of the baseline samples in Figure 10.

The tested CVD graphene samples are shown in Figure 11a. After 24 h of testing four out of the seven samples were entirely corroded. After 48 h of testing the remaining three samples corroded as well. Interestingly, the corrosion rate was significantly higher than the corrosion rate of the pristine ZnNi plates in Figure 10. A possible mechanism responsible for this behavior is the galvanic effect between the dissimilar layers of the ZnNi and graphene in the presence of the sodium chloride (NaCl) electrolyte. The mitigation of the galvanic corrosion must be further investigated.

Steel plates: The samples 1-15 were coated with SH silica and thereafter were impregnated with exfoliated GnPs in the polydimethylsiloxane matrix. The images of the samples after the completion of 240 h of testing are shown in Figure 11b. The metallic substrate of the samples 2-5 is steel without ZnNi. The samples that are based on DE and micron size spherical silica (2, 4, and 5) were corroded. Sample 3, is based on nanometer size spherical silica and showed minimal signs of corrosion.

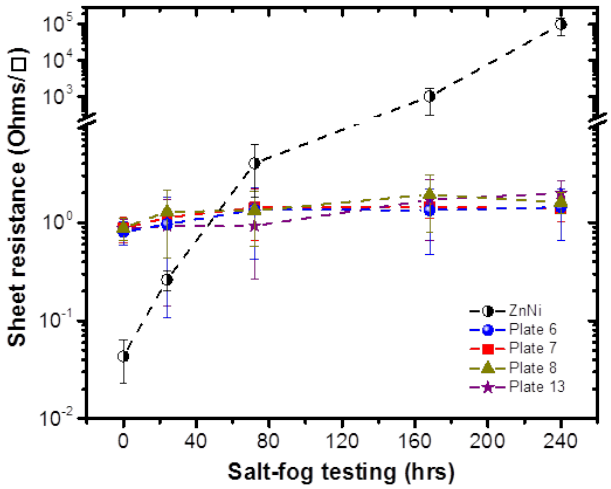

Figure 12. Sheet resistance values of the best performing coatings and of the ZnNi plate as a function of the salt-fog testing.

ZnNi plates: Unlike the samples in Figure 11a, the coated ZnNi samples (plates 6-15) showed excellent corrosion resistance. No visual signs of corrosion were observed. This can be attributed to the silica component of the coatings that forms a barrier between the dissimilar ZnNi and graphene layers and therefore is anticipated to protect the substrates from the galvanic effects. The sheet resistance values of the best performing coatings versus the salt-fog exposure are summarized in Figure 12. The sheet resistance of the ZnNi plate started to increase within the first 24 h of testing. After 50 h of testing the sheet resistance was higher than the sheet resistance of the coated plates. Increase in the salt-fog exposure time of the plates resulted in the formation of a non-conductive layer on the ZnNi surface and the sheet resistance of the plate rapidly increased to 10^5 Ω/sq. On the contrary, the sheet resistance of the coated plates 6, 7, 8, and 13 was approximately 1 Ω/sq during the entire testing period. For the given testing period, this is a ten-fold increase in the corrosion resistance of the developed coatings in regard to the onset of the sheet resistance values and therefore to the onset of the corrosion formation. The coated plates in Figure 12 are based on the nanometer size silica particles that are shown in Figure 5. Compared to the coatings based on micron size DE or micron size silica particles, the coatings based on nanometer size silica showed superior performance. The smaller size of the particles may have resulted in coatings

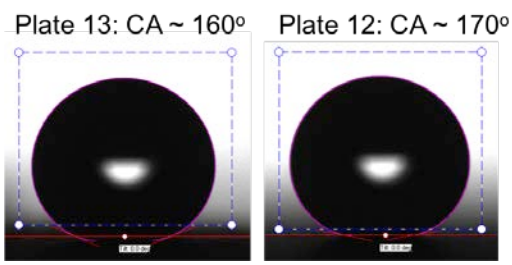

(a)

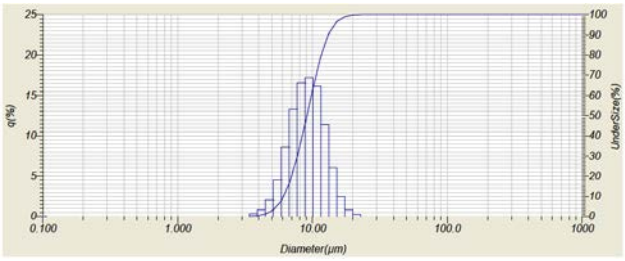

(b)

Figure 13. (a) The CA of the best coating (plate 13) is approximately 160º. The coating based on micron size silica (i.e. plate 12) has the highest CA that is approximately 170º. However, their sheet resistance values are not consistent. **(b)** Particle size analysis of the micron size spherical silica. The mean size is 9.2 ± 2.8 μm.

with lower porosity and a more uniform (defect-free) particle distribution on the plate's surface. The interdependence between the porosity and the corrosion resistance of the coatings must be further investigated.

Plate 13 is the only SH plate among the coated plates in Figure 12. The contact angle (CA) values were approximately 160^o during the entire testing period. Plate 6 was marginally SH with CA values ranging between 140^o and 150^o. Plates 7 and 8 are hydrophobic with CA values approximately 120^o. The coatings that were based on micron size silica demonstrated the highest CA values (~ 170^o). Representative CA measurements are shown in Figure 13. However, these coatings were either non-conductive or the sheet resistance values were inconsistent across their surface. Based on our testing results the best formulation is coating 13. The resistance of this coating must further be improved.

5. Conclusions and Implications for Future Research

We developed anticorrosion coatings based on assemblies of *i)* single atom graphene layers and *ii)* exfoliated graphene nanoplatelets (GnPs) in polydimethylsiloxane and superhydrophobic (SH) diatomaceous earth and silica particles of different sizes and geometries. In order to optimize the formulation of the coatings, thirty zinc-nickel (ZnNi) and steel plates were coated using different combinations of silica particles and GnPs. The samples were subjected to salt-fog testing according to ASTM B-117 and their sheet resistance and SH properties were evaluated. The assembly of a few single atom graphene layers on top of the ZnNi was found to significantly accelerate the corrosion process probably due to galvanic effects. One the contrary, the assemblies of GnPs, and SH silica particles demonstrated excellent corrosion resistance. The coatings based on spherical SH silica with 300 nm diameter were found to have the lowest sheet resistance (~ 1 Ω/sq) over the entire testing period (240 h). The sheet resistance of the pristine ZnNi plate started to increase within the first 24 h of testing. Our best performance coating demonstrated a ten-fold increase in the corrosion resistance compared to the ZnNi coating. The coating remained SH over the entire testing period. The best performance coating was applied on electrical backshell connectors. The connectors were SH and corrosion free after 240 h of salt-fog testing. The developed coatings are inexpensive and can be applied on ZnNi coatings in order to extend their corrosion resistance and make it comparable to the corrosion resistance of coatings that are based on hexavalent chromium and cadmium. The proof-of-concept has been demonstrated: The synergistic effects of the water repellency, and moisture and oxygen barrier resulted in an impermeable coating that protected metal components from corrosion. The coated components demonstrated superior corrosion resistance compared to the respective steel and ZnNi components.

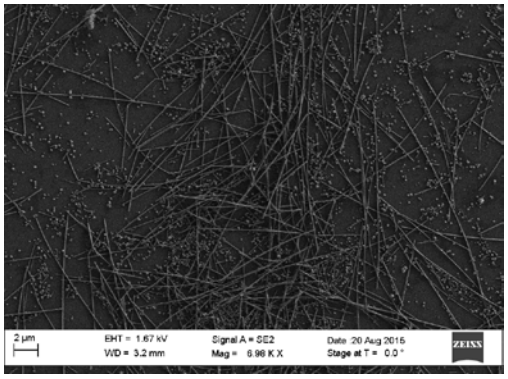

Figure 14. High aspect ratio silver nanowires synthesized in our group using sol-gel techniques.

Future Research

The proof-of-concept regarding the corrosion resistance of the developed coatings has successfully been demonstrated (Figure 12). The electrical resistance of the coatings should further be decreased

in order to reach the mΩ range. A proposed method to decrease the electrical resistance of the coatings is to use a conductive polymer matrix and disperse high aspect ratio silver nanowires into the coating formulations. The electrical resistance will substantially decrease when the nanowire content is above the percolation threshold. The latter is anticipated to be reached even at low volume fractions because of the high aspect ratio of the nanowires. High aspect ratio silver nanowires that are synthesized in our group using sol-gel techniques are shown in Figure 14.

Based on our results the developed type of coating can be a beneficial component in corrosion preventive compounds. Additional testing and development is required to evaluate the performance of the coatings and assess the degradation mechanisms. We propose to study the galvanic mechanism and the scratch resistance of the coatings in order to mitigate the galvanic effect. The abrasion and UV resistance of the coatings should also be evaluated. The resistance of the coatings can be further improved. This type of coating can also provide water displacement and be utilized as a component in corrosion preventive compounds.

6. Literature Cited

1. Feng XJ, Jiang L. "Design and creation of superwetting/antiwetting surfaces" Adv. Mater. 18, 3063–3078 (2006).

2. D'Urso B, Simpson JT, Kalyanaraman M. "Emergence of superhydrophobic behavior on vertically aligned nanocone arrays" Appl. Phys. Let. 90, 044102 (2007).

3. Polizos G, Tuncer E, Qiu X, Aytug T, Kidder MK, Messman JM, Sauers I. "Nonfunctionalized polydimethyl siloxane superhydrophobic surfaces based on hydrophobic-hydrophilic interactions" Langmuir 27, 2953–2957 (2011).

4. Genzer J, Efimenko K. "Recent developments in superhydrophobic surfaces and their relevance to marine fouling: a review" Biofouling 22, 339–360 (2006).

5. Landoulsi J, Cooksey KE, Dupres V. "Interactions between diatoms and stainless steel: focus on biofouling and biocorrosion" Biofouling 27, 1105–1124 (2011).

6. Simons SJR. "Modelling of agglomerating systems: From spheres to fractals" Powder Technol. 87, 29–41 (1996).

7. Polizos G, Winter K, Lance MJ, Meyer HM, Armstrong BL, Schaeffer DA, Simpson JT, Hunter SR, Datskos PG. "Scalable superhydrophobic coatings based on fluorinated diatomaceous earth: Abrasion resistance versus particle geometry" Appl. Surf. Sci. 292, 563–569 (2014).

8. Vlassiouk I, Regmi M, Fulvio P, Dai S, Datskos P, Eres G, Smirnov S. "Role of Hydrogen in Chemical Vapor Deposition Growth of Large Single-Crystal Graphene" ACS Nano 5, 6069–6067 (2011).

9. Vlassiouk I, Fulvio P, Meyer H, Lavrik N, Dai S, Datskos P, Smirnov S. "Large scale atmospheric pressure chemical vapor deposition of graphene" Carbon 54, 58–67 (2013).

10. K.R. Paton et al., “Scalable production of large quantities of defect-free few-layer graphene by shear exfoliation in liquids” Nature Materials 13, 624-630 (2014).

11. Thermo Scientific Application Note AN52252 “The Raman Spectroscopy of Graphene and the Determination of Layer Thickness” by Mark Wall, Thermo Fisher Scientific, Madison, WI, USA.